The collective excitations of normal and superfluid ^{4}He: the dependence on pressure and temperature

1999 J. Phys.: Condens. Matter 11 603

(http://iopscience.iop.org/0953-8984/11/3/003)

J. Phys.: Condens. Matter **11** (1999) 603–628. Printed in the UK PII: S0953-8984(99)97081-9

The collective excitations of normal and superfluid ^{4}He: the dependence on pressure and temperature

M R Gibbs†‡‖, K H Andersen§, W G Stirling‡ and H Schober§

† Department of Physics, University of Keele, Keele ST5 5BG, UK
‡ Oliver Lodge Laboratory, Department of Physics, University of Liverpool, Liverpool L69 7ZE, UK
§ Institut Laue–Langevin, Avenue des Martyrs, BP156, 38042 Grenoble Cédex 9, France

Received 1 September 1998, in final form 20 October 1998

Abstract. Systematic high-resolution measurements of the collective excitations in normal and superfluid ^{4}He have been made as a function of both pressure (density) and temperature using neutron inelastic scattering. The IN6 time-of-flight spectrometer at the Institut Laue–Langevin has been used to obtain accurate and consistent data over a wavevector range $0.3 < Q < 2.35$ Å^{-1}. We present and discuss the experimental data. An analysis, based on the simple-subtraction model, is made; single-excitation energies, widths, and magnitudes are extracted. Many changes in the excitations are shown to occur at the λ-transition. The single excitations are discussed in the light of current theory. The structure of the multiphonon continuum and its dependence on pressure is also discussed.

1. Introduction

Sharp, well defined, collective excitations with a roton minimum are associated with the superfluid phase of liquid ^{4}He [1]. Neutron inelastic scattering allows direct observation of these excitations. We refer the reader to the monographs by Griffin [2] and Glyde [3] for overviews of the many experimental and theoretical studies of these excitations to date.

The pressure and temperature dependence of the collective excitations in ^{4}He have been measured using time-of-flight neutron inelastic scattering on the IN6 spectrometer at the Institut Laue–Langevin, Grenoble. This work is intended as a continuation and completion of the previous study of the temperature dependence of the collective excitations of superfluid ^{4}He at saturated vapour pressure (SVP) made by Andersen *et al* [4], and Andersen and Stirling [5], again using the IN6 spectrometer (these studies are hereafter collectively referred to as those of AS). The present study, combined with that of AS, gives a consistent investigation of the dynamic structure factor, $S(Q, E)$, over a substantial part of the normal and superfluid phase diagram under near-identical resolution conditions. Particular attention was paid to studying the superfluid phase, especially near the λ-transition where most of the changes to the excitations occur. The measurements therefore complement those of Svensson *et al* [6] which specifically focus on the changes to the excitations at the λ-transition, and those of Crevecoeur [7] which focus on ^{4}He in the normal-fluid phase. The temperature dependence study by AS at SVP has been frequently used for comparison to theoretical predictions [2, 3]. It is intended that this extension of their study to higher pressures will be similarly useful.

‖ Present address: Department of Physics, University of Exeter, Stocker Road, Exeter, Devon EX4 4QL, UK.

0953-8984/99/030603+26$19.50

In this paper experimental data are presented and a detailed lineshape analysis is made. The simple-subtraction method due to Miller *et al* [8] was used to separate the single-phonon and multiphonon excitations. The validity of other analytical methods (such as the Woods and Svensson [9] decomposition) is discussed. In addition, the multiphonon excitations are presented and discussed.

The effect of pressure on the excitations at low temperature has been studied previously [10–13]. In the phonon region the gradient of the dispersion ($\mathrm{d}E_Q/\mathrm{d}Q$) is larger at pressure, in accord with the increase in the first-sound (a longitudinal density wave) velocity, c. The effects of anomalous (or upward) dispersion in the phonon region decrease with pressure [14]. The excitation energies increase with pressure for wavevectors up to nearly the roton minimum [10]; thereafter they decrease. The wavevector of the roton minimum Q_R is larger at pressure [11].

Previous high-resolution studies of the temperature dependence of the collective excitations at pressure (only at maxon and roton wavevectors) [15] helped lead to the development of the density–quasiparticle model of Glyde and Griffin [16]; this model implies a link between the collective excitations and Bose–Einstein condensation. Although no direct comparison of this model was made to the data in this study, significant changes are seen to occur at the λ-transition at all pressures; this implies that the excitations are indeed related to Bose–Einstein condensation.

2. Experimental details

Experimental data were collected using the IN6 direct-geometry (fixed incident neutron wavelength) neutron inelastic spectrometer at the Institut Laue–Langevin, Grenoble. The incident neutron wavelength was set to $\lambda_i = 4.153$ Å ($E_i = 4.877$ meV), allowing simultaneous detection over the entire superfluid ^{4}He phonon–roton dispersion relation in a single measurement. Figure 1 shows the region of Q–E space covered. In this study, the chosen incident neutron wavelength was shorter than that used by AS (who set $\lambda_i = 4.63$ Å); while their longer incident wavelength gave a narrower resolution than the present study, it would not have allowed study of the entire phonon–roton dispersion relation when the helium was at higher pressure (where the roton wavevector is increased).

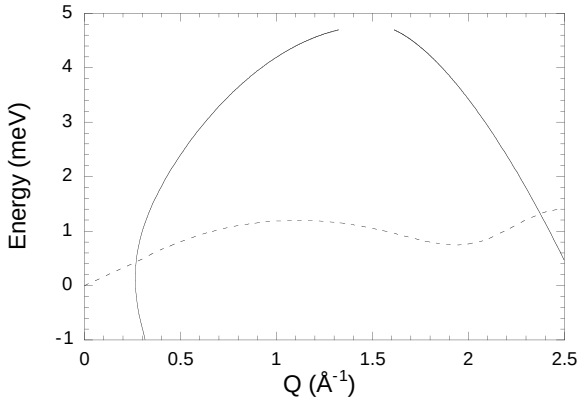

Figure 1. The region of Q–E space observed simultaneously on the IN6 spectrometer with an incident neutron energy of 4.877 meV. The region is delimited by the loci—through Q–E space—of constant scattering angle of the highest and lowest detector angles (solid lines). The dotted line is the superfluid phonon dispersion relation at SVP [4, 5].

The cylindrical aluminium sample cell had an internal diameter of 2.6 cm, a height of 4 cm, and a wall thickness of 0.3 cm. A system of cadmium discs, mounted horizontally inside the cell and spaced 1 cm apart, reduced multiple scattering. The sample volume was approximately 21 cm^3. High-purity (99.999%) ^{4}He was condensed into the sample cell, mounted in a ^{3}He-flow cryostat. The cryostat gave good temperature stability in the range $0.4 < T < 4$ K. Before it was condensed, the ^{4}He gas was passed through a liquid-nitrogen-cooled trap to 'freeze out' remaining impurities. The cold trap consisted of a U-shaped tube approximately 50 cm long and 2 cm diameter; this was packed with charcoal sinter giving a large internal surface area.

The scattering function of ^{4}He was measured at 0.5 K (just above the cryostat's base temperature) at six different pressures: SVP, 2, 5, 10, 15, and 20 bar. Of these pressures, the full temperature dependence in the normal and superfluid phases was measured at 5, 10, and 20 bar. The counting time for each measurement was approximately four hours; during this time of the order of 10^9 neutrons were incident to the sample, enough for obtaining data with good statistical precision. Empty-sample-cell data were taken at $T < 4$ K and the observed scattering is entirely elastic. The empty-sample-cell data were subtracted from the observed helium data.

The data were converted to $S(Q, E)$ on an absolute scale using standard time-of-flight data-reduction techniques and then rebinned to constant Q. For more details see Gibbs [17]. Care was taken to minimize systematic errors in both the measurement and in the data-reduction process. Typical vanadium (elastic) scattering resolution widths were ≈0.12 meV (FWHM). The Q-dependent helium resolution widths varied between typically 0.09 and 0.16 meV (FWHM).

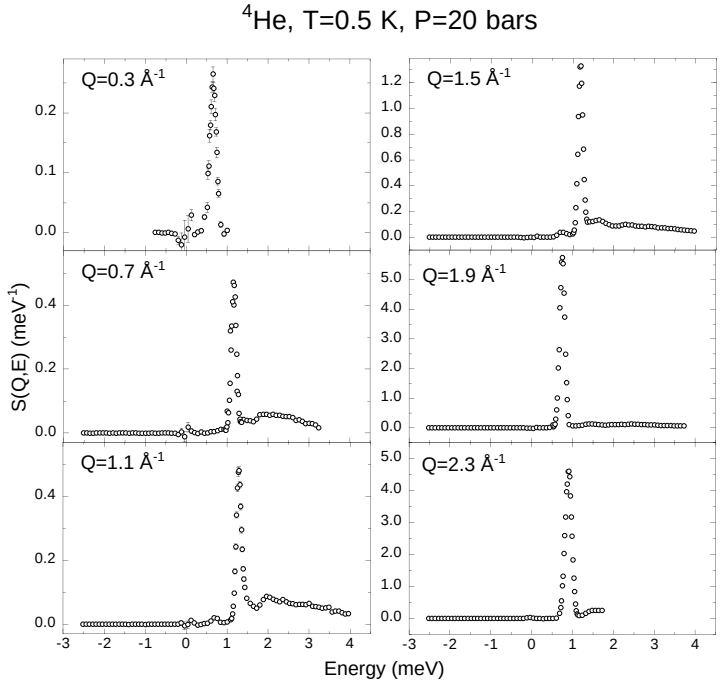

Figure 2. Typical low-temperature ^{4}He data rebinned to constant Q. $T = 0.5$ K, $P = 20$ bar. The increased errors near $E = 0$ arise from the subtraction of the (elastic) empty-cell scattering.

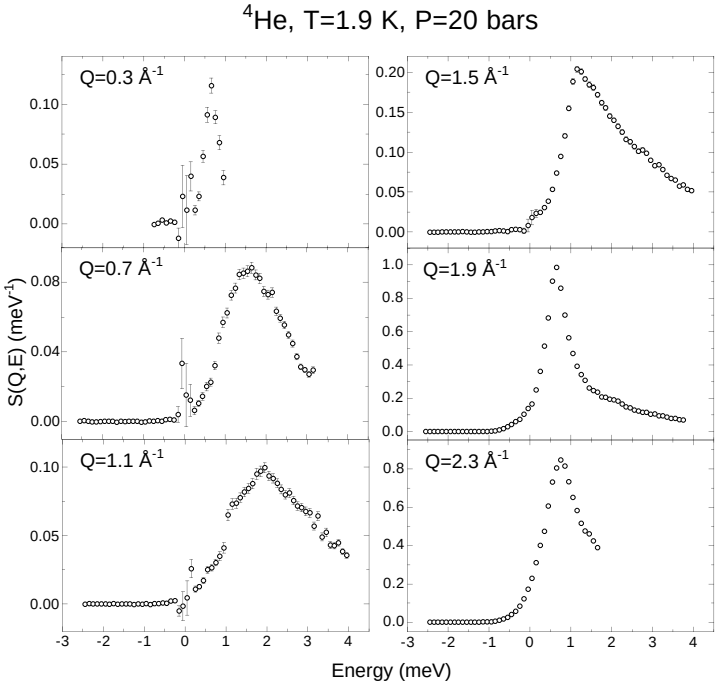

Figure 3. Typical ^{4}He data just below the λ-transition, rebinned to constant Q. $T = 1.9$ K, $P = 20$ bar. The increased errors near $E = 0$ arise from the subtraction of the (elastic) empty-cell scattering.

3. Presentation of experimental data

Typical constant-Q data at 20 bar are shown in figures 2–4. The low-temperature (0.5 K) data (figure 2) are always composed of a single, sharp peak (the phonon–roton excitation) superimposed on a broad 'multiphonon' scattering feature. Figure 3 shows typical scattering at 1.9 K, just below $T_\lambda = 1.928$ K at 20 bar†. Although a single-excitation peak remains distinct from the multiphonon scattering, it has broadened significantly. At 2.5 K—above T_λ—all of the scattering (figure 4) is a broad function of energy, and the scattering is largely featureless. The scattering from the normal fluid is very similar to the scattering seen from other low-temperature liquids [18].

The data presented in this study are tabulated in appendix A of Gibbs [17].

3.1. The pressure dependence of the low-temperature data

The pressure dependencies of the observed $S(Q, E)$ in the phonon ($Q = 0.4$ Å^{-1}), maxon ($Q = 1.2$ Å^{-1}), and roton ($Q = 2.0$ Å^{-1}) regions at 0.5 K are shown in figure 5. The pressure dependence of the excitations in the phonon region (figure 5, upper panel) confirm expectations: a single, sharp peak is present, the energy of which increases with pressure. This is consistent with expectations of a first-sound mode whose velocity ($\mathrm{d}E/\hbar\,\mathrm{d}Q\lim_{Q\to 0}$) increases with density. The peak height decreases with increasing pressure indicating that

† The superfluid transition temperature, T_λ, is dependent on pressure. At SVP, $T_\lambda = 2.172$ K; at 2 bar, $T_\lambda = 2.154$ K; at 5 bar, $T_\lambda = 2.122$ K; at 10 bar, $T_\lambda = 2.063$ K; at 15 bar, $T_\lambda = 1.998$ K; and at 20 bar, $T_\lambda = 1.928$ K.

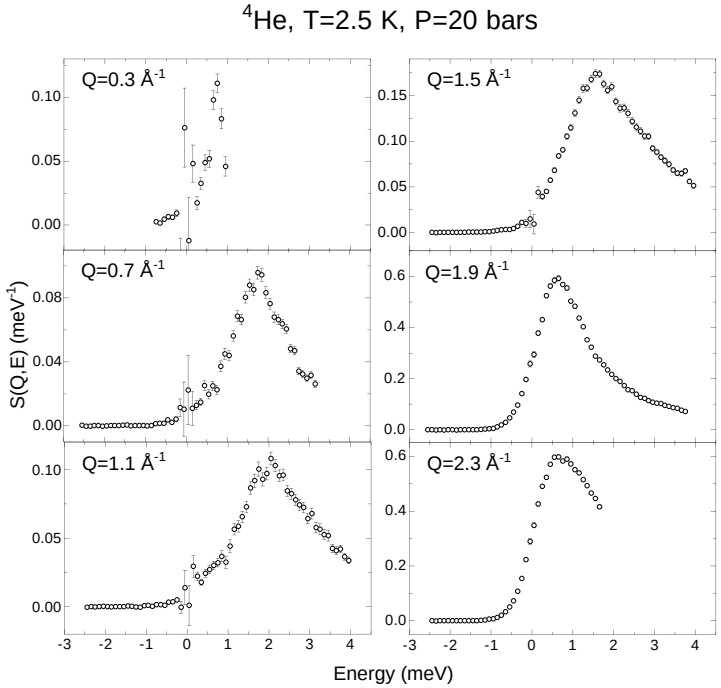

Figure 4. Typical ^{4}He data in the normal-fluid phase, rebinned to constant Q. $T = 2.5$ K, $P = 20$ bar. The increased errors near $E = 0$ arise from the subtraction of the (elastic) empty-cell scattering.

interactions between single-phonon and multiphonon excitations may be stronger in the fluid at increased density. The measurements in the phonon region do not extend very high in energy (up to 1.8 meV) due to kinematical restrictions. However, multiphonon scattering in the phonon region is weaker than in other wavevector regions [19]. The multiphonon excitations are discussed in a later section.

As was the case with the phonon excitations, the single excitations in the maxon wavevector region also decrease in intensity with increasing pressure (figure 5, centre panel). The maxon excitation does not broaden with increasing pressure, indicating that any possible decay process into pairs of rotons does not occur. Confirming the results of Dietrich *et al* [10], the single-roton excitation is sharp and is a very prominent feature of $S(Q, E)$ at all pressures (figure 5, lower panel). The peak position of the roton decreases with increasing pressure and the peak intensity increases.

3.2. The temperature dependence of the 20 bar data

The temperature dependence of the observed $S(Q, E)$ at 20 bar (figure 6) typifies the temperature dependence close to the solidification pressure of ^{4}He (25 bar). We therefore focus this study on the excitations at 20 bar pressure. The temperature dependence of the phonon excitation ($Q = 0.4$ Å^{-1}) at 20 bar (figure 6, upper panel) remains, in many respects, similar to that at SVP; the low-temperature (0.5 K) scattering consists of a single, sharp peak which broadens with increasing temperature. The rate of excitation broadening with temperature is small at low temperatures and increases as the λ-transition is approached. Above T_λ there is

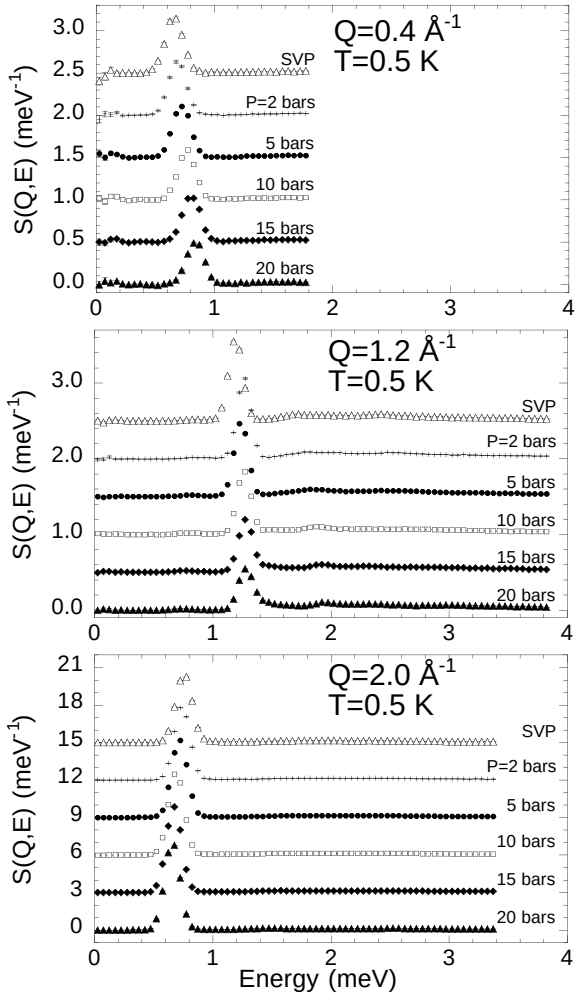

Figure 5. The pressure dependence of constant-Q data; $T = 0.5$ K. Upper panel, $Q = 0.4$ Å^{-1}. Centre panel, $Q = 1.2$ Å^{-1}. Lower panel, $Q = 2.0$ Å^{-1}.

little change in the phonon width, and most changes to the profile of $S(Q, E)$ are due to the Bose detailed-balance factor. A change in the phonon excitation peak position is observed at the λ-transition. Although this change in the peak position has been observed in previous studies [5, 6, 20], it is noted here that it is much more pronounced at pressure. Above T_λ the peak position remains essentially constant.

At the maxon wavevector (figure 6, centre panel), the low-temperature single excitation is superimposed on a (largely temperature-independent) multiphonon background. The narrow single peak broadens and decreases in intensity with increasing temperature. Above T_λ it has disappeared entirely.

Although the single-roton peak is a factor of ten more intense than the maxon, its temperature dependence is very similar (figure 6, lower panel): the sharply peaked single excitation, superimposed on a multiphonon background, also broadens with increasing

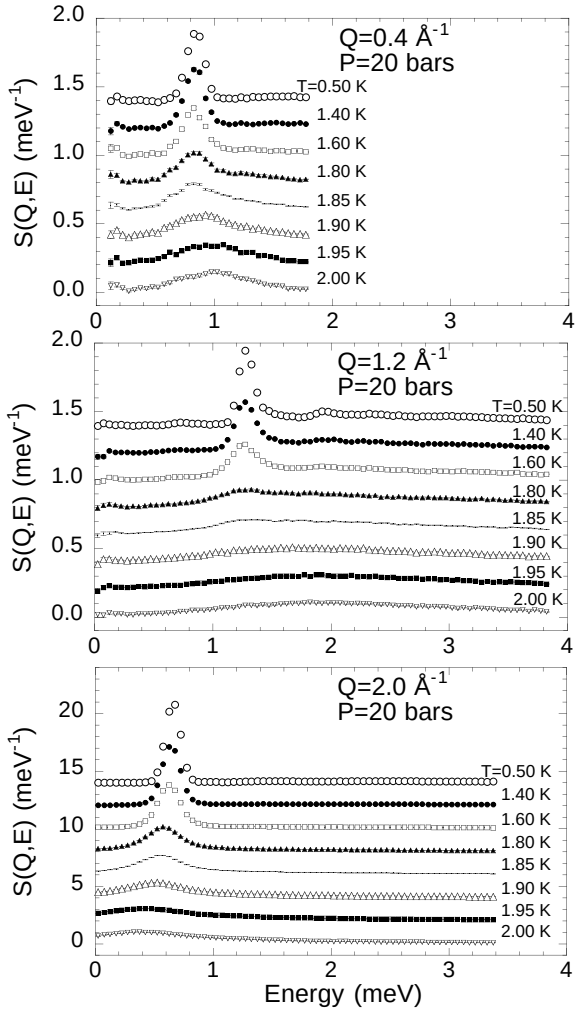

Figure 6. The temperature dependence of constant-Q data at $P = 20$ bar. Upper panel, $Q = 0.4$ Å^{-1}. Centre panel, $Q = 1.2$ Å^{-1}. Lower panel, $Q = 2.0$ Å^{-1}.

temperature below T_λ, and disappears abruptly at the λ-transition. In the normal phase, the remaining broad scattering is peaked at an energy considerably lower than that of the single sharp peak observed in the superfluid.

4. Modelling and parametrization of the experimental data

4.1. The damped harmonic oscillator lineshape

The single-phonon–roton excitations may be modelled by a response function similar to that normally used to describe damped harmonic phonons in solids. The theory of undamped normal modes of vibration in a material gives a scattering cross section with a delta-function in the energy transfer [21]. A sharp peak will be observed, therefore, in a neutron inelastic

scattering experiment at a neutron energy transfer equal to the energy (frequency) of a normal mode at the observed wavevector. However, at finite temperatures interactions between excitations are possible. These interactions lead to a finite excitation lifetime, broadening the excitations in frequency (energy), and to a shift in energy. In the small-excitation-lifetime limit (i.e. the excitation width $\Gamma_Q \ll E_Q$, the single-collective-mode energy), the damped harmonic oscillator (DHO) expression (shown below) is a valid model of single collective modes in superfluid ^{4}He [20, 22]:

$$S_1(Q, E) = \frac{Z_Q}{\pi}\,[n_B(E) + 1]\left[\frac{\Gamma_Q}{(E - E_Q)^2 + \Gamma_Q^2} - \frac{\Gamma_Q}{(E + E_Q)^2 + \Gamma_Q^2}\right] \qquad (1)$$

where Z_Q is the single-excitation weight, Γ_Q the excitation half-width at half-maximum (HWHM), and E_Q the excitation energy. In this study we choose E_Q to represent the excitation energy, rather than $\sqrt{E_Q^2 + \Gamma_Q^2}$ as suggested by other authors [22–24]. n_B is the Bose distribution function. The origin of the DHO response function, and its relation to the single-particle Green's function of the liquid, is outlined in appendix C of Glyde [3].

There is, however, little theoretical justification for the application of the DHO expression at higher temperatures where the lifetime of single excitations is greatly diminished and Γ_Q is of the same order as E_Q (this occurs near T_λ for the roton). The DHO loses further validity at increased widths because, to make model fitting tractable, it is usually assumed that Γ_Q is independent of energy. Also, the DHO function in no way allows for the possibility that the excitations in the superfluid could be of a fundamentally different origin to the normal-fluid excitations. Despite the above disadvantages, the DHO function has been shown in many previous studies to characterize well the single excitations of both normal and superfluid ^{4}He at all temperatures; it remains the only consistent and generally accepted parametrization of the single-excitation energies, widths, and mode strengths.

It is important to allow for the effects of the finite instrumental resolution. Since the resolution depends on both Q and E, we have chosen to use the lowest-temperature (0.5 K) energy widths to represent the instrumental contribution at each wavevector and pressure. At SVP, where the excitation widths are very small at low temperatures ($\sim\mu$eV), this is certainly an adequate approximation. The measured widths of the 20 bar data show no significant broadening effects that can be attributed to the increased pressure; on average, the widths are very similar to (or smaller than) those at SVP. To extract the excitation parameters (energy, width, and weight), the DHO function was convoluted with a Gaussian function of the appropriate resolution width at each wavevector.

4.2. Decomposition of single-phonon and multiphonon contributions to S(Q, E)

The DHO function described above models the single-excitation response of liquid ^{4}He. It does not, however, describe the creation of more than one excitation in a single scattering event. This 'multiphonon' scattering is an inherent component of the dynamic structure factor $S(Q, E)$ and exists irrespective of the instrumentation. Several decompositions of the observed scattering into single-phonon and multiphonon components have been proposed. In the two-fluid model proposed by Woods and Svensson [9], single-phonon and multiphonon components scale with the superfluid and normal-fluid densities, ρ_S and ρ_N, respectively. The Woods and Svensson model gives a reasonable representation of the temperature dependence of $S(Q, E)$ at SVP [9, 4, 5]. However, in detailed studies by Talbot *et al* [15] and AS, the model resulted in unphysical oversubtractions of the normal (multiphonon) component. For this reason it was decided to use the simple-subtraction (SS) model first proposed by Miller *et al* [8]. The SS model also makes no prior assumptions relating the excitations to superfluidity.

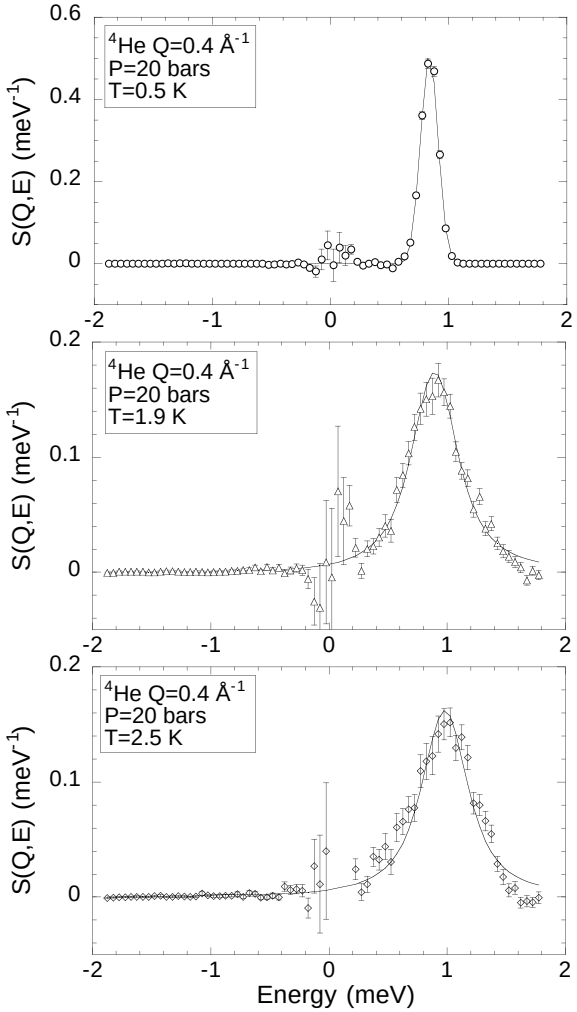

Figure 7. Spectra fitted with damped harmonic oscillator functions at $Q = 0.4$ Å^{-1}, $P = 20$ bar. The single-excitation peaks were extracted using the simple-subtraction method; fits to the single peak only are indicated by the solid curves.

The SS form describes the total scattering as the sum of two components, the single-excitation dynamic structure factor $S_1(Q, E)$, and the multiphonon dynamic structure factor $S_M(Q, E)$. The multiphonon component is assumed to be independent of temperature. Experimentally, the multiphonon scattering is found to vary only relatively weakly with temperature. Hence, at all temperatures,

$$S(Q, E; T) = S_1(Q, E; T) + S_M(Q, E). \tag{2}$$

The multiphonon component $S_M(Q, E)$ is extracted from the lowest-temperature data (in this case, those for 0.5 K) where it is most clearly separated from the single-excitation peak. This same multiphonon component is then subtracted from higher-temperature data, revealing what is assumed to be the (now broader) single excitation. However, Talbot *et al* [15] and Stirling and Glyde [20] have noted the oversimplification of assuming the multiphonon excitations to

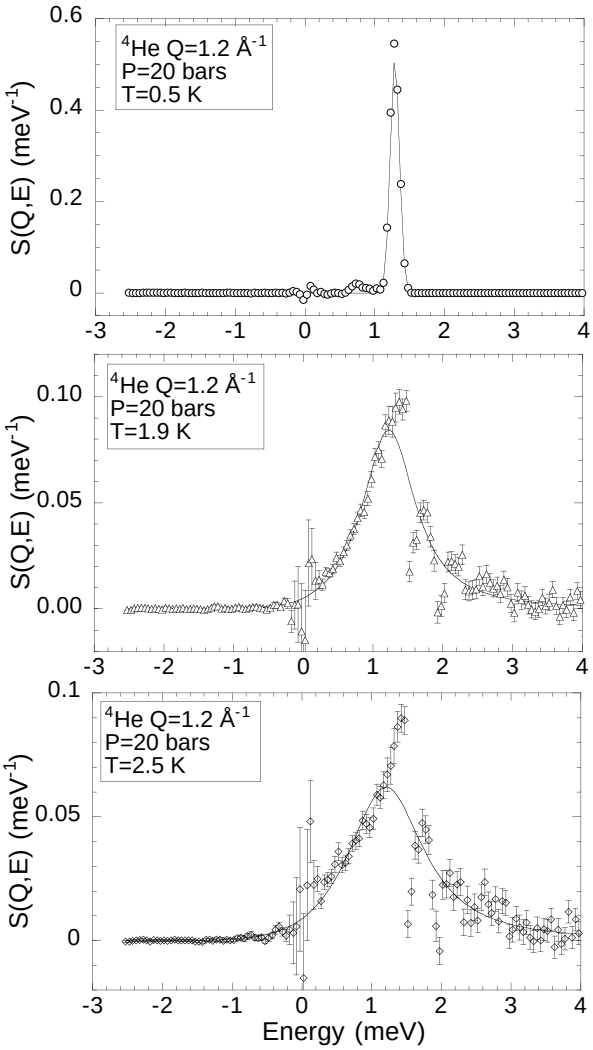

Figure 8. Spectra fitted with damped harmonic oscillator functions at $Q = 1.2$ Å^{-1}, $P = 20$ bar. The single-excitation peaks were extracted using the simple-subtraction method; fits to the single peak only are indicated by the solid curves.

be entirely independent of temperature. If the single-phonon scattering at high temperature is characteristically broader, inevitably the multiphonon scattering will be less structured. In addition, the SS model does not allow for possible interference and hybridization between single-phonon and multiphonon excitations [3]; these effects may be more prominent at higher pressure.

Notwithstanding these reservations, the SS method remains a useful and simple method (as its name implies) of extracting the single excitations in normal and superfluid ^{4}He. It introduces relatively little model dependence to the parameters obtained, accounting for the multiphonon excitations without biasing systematic changes at the λ-transition. The SS model was used, therefore, to analyse the temperature-dependent data at pressure in this study. Typical fitted lineshapes can be seen in figures 7–9.

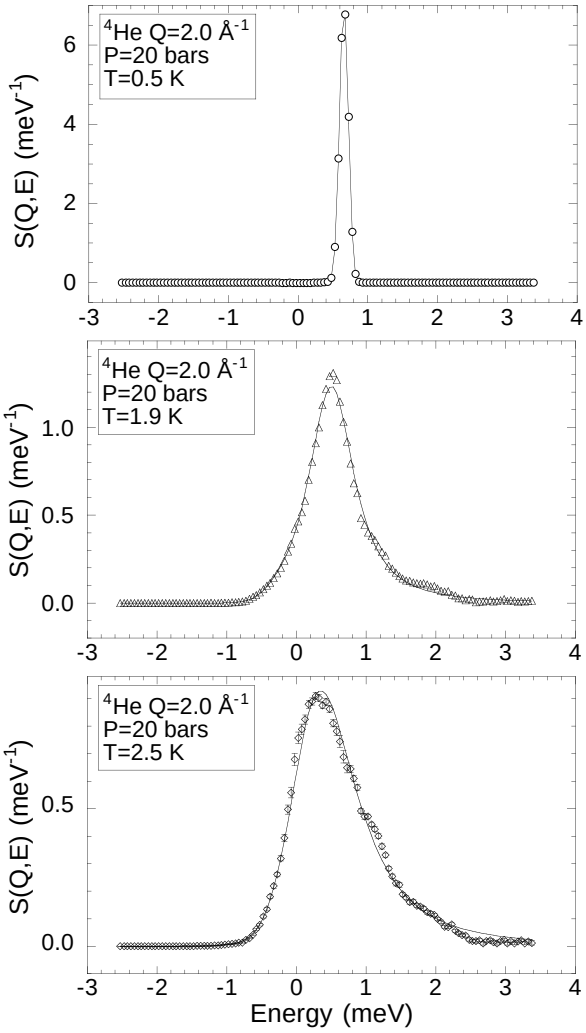

Figure 9. Spectra fitted with damped harmonic oscillator functions at $Q = 2.0$ Å^{-1}, $P = 20$ bar. The single-excitation peaks were extracted using the simple-subtraction method; fits to the single peak only are indicated by the solid curves.

Using the SS method, the DHO function fitted well at all pressures for temperatures below 1.6 K. The reduced χ^2-values of the least-squares fits were between 1.0 and 2.5. However, at higher temperatures the multiphonon excitations contained in $S_M(Q, E)$, extracted at 0.5 K, represent the true multiphonon component of $S(Q, E)$ less accurately. This is reflected in the very poor continuity seen at 1.9 K and 2.5 K in the maxon region (figure 8, middle and lower panels). Above 1.6 K the DHO function fitted less well. Indeed, as discussed above, at these temperatures use of the DHO function is less justifiable as $\Gamma_Q \sim E_Q$. The fitted lineshape and the extracted parameters may still be said, however, to be 'characteristic' of the data. For comparison, the DHO function was fitted to the observed scattering above T_λ with no correction for the multiphonon component. The resultant lineshape, while fitting the low-energy side of the peak, underestimated the intensity in the high-energy tail.

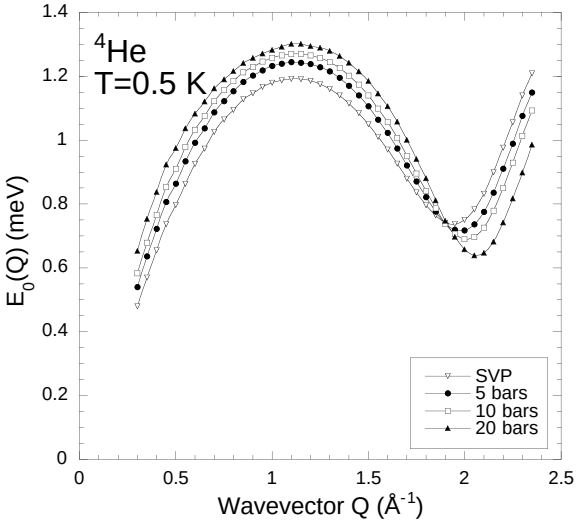

Figure 10. The wavevector dependence of the single-excitation energies E_Q at $T = 0.5$ K. Data at SVP, and 5, 10, and 20 bar pressure are shown. The solid curves are a guide to the eye.

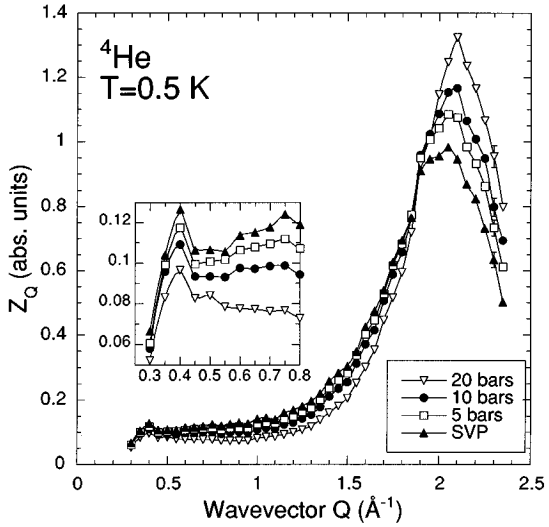

Figure 11. The wavevector dependence of the single-excitation weights Z_Q at $T = 0.5$ K. Data at SVP, and 5, 10, and 20 bar are shown. The inset highlights the wavevector dependence of Z_Q in the phonon region. The solid curves are a guide to the eye.

5. The pressure dependence of the fitted DHO parameters at low temperature

We present the pressure dependence of the DHO parameters fitted to the experimental data at 0.5 K. Figure 10 shows the wavevector dependence of the excitation energies E_Q as a function of pressure at low temperature (0.5 K). The familiar phonon–roton dispersion relation is clearly observed and this is dependent on pressure. The pressure dependence of the single-phonon

weight Z_Q at 0.5 K is shown, as a function of Q, in figure 11; the data are in reasonable accord with previous (lower-intensity and poorer-resolution) measurements [10].

It is a long-standing puzzle why Z_Q has two apparent maxima, one in the roton region (see figure 11), and another (smaller peak) in the phonon region (see the inset of figure 11). Cowley and Woods [25] first commented on this. Griffin and Svensson [26] suggest that the double maxima may be interpreted—within the context of the Glyde–Griffin [16] model—as arising from two separate contributions to $S(Q, E)$, a regular density mode (at low Q) and the single-quasiparticle mode (at higher Q between the maxon and the roton). Further theoretical and experimental studies are needed to confirm this interpretation.

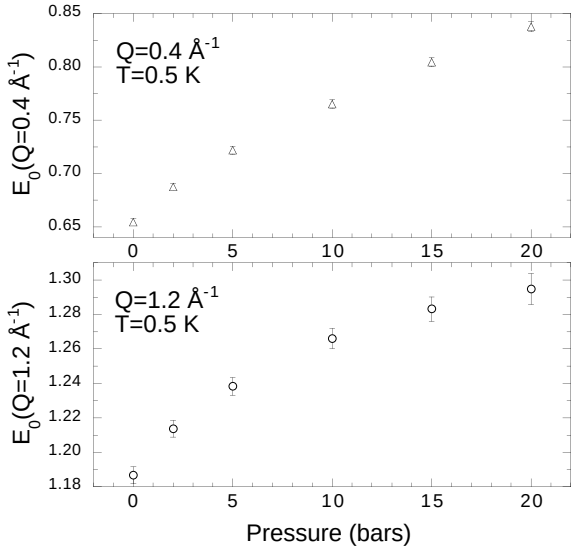

Figure 12. The pressure dependence of the excitation energies E_Q in the phonon region (upper panel) and at the maxon (lower panel). $T = 0.5$ K.

5.1. The pressure dependence of the fitted DHO parameters in the phonon region

The pressure dependence of $S(Q, E)$ in the phonon region at low temperature is consistent with previous neutron scattering measurements [13, 19] and ultrasound measurements [27]. Less anomalous dispersion is present at higher pressure [28] and the anomalous dispersion cut-off wavevector, Q_C, diminishes [29]. The data observed in this study do not, however, extend to wavevectors low enough (observed $Q \geqslant 0.3$ Å^{-1}) to make any further investigation into the pressure dependence of the anomalous dispersion. The upper panel of figure 12 shows the pressure dependence of the phonon energy. The full width at half-maximum of the phonon excitations, $2\Gamma_Q$, remains negligible in comparison to the resolution width.

5.2. The pressure dependence of the fitted DHO parameters in the maxon region

The maxon excitation is of particular interest because interference and hybridization between single-phonon and multiphonon excitations are expected to be strong—at pressure—in this, the highest-energy region of the dispersion relation. The pressure dependence of the maxon energy E_Q can be seen in the lower panel of figure 12. Although no intrinsic broadening is

observed in the maxon region at low temperature, the single-excitation weight Z_Q diminishes with pressure at the maxon (see the inset of figure 11). This may indicate 'anharmonic' effects; although no precise formulation of anharmonic collective density excitations in liquids exists at present, we note the similarity between the single-excitation contributions for liquid ^{4}He and bcc solid ^{4}He (reference [3], page 232). In agreement with Svensson *et al* [30], the pressure dependence of Z_Q at the maxon is approximately linear and shows no signs of inflection or discontinuity when the maxon energy exceeds 2Δ (at $P \approx 19$ bar). The decay of single-maxon excitations into pairs of rotons is not, therefore, a significant process.

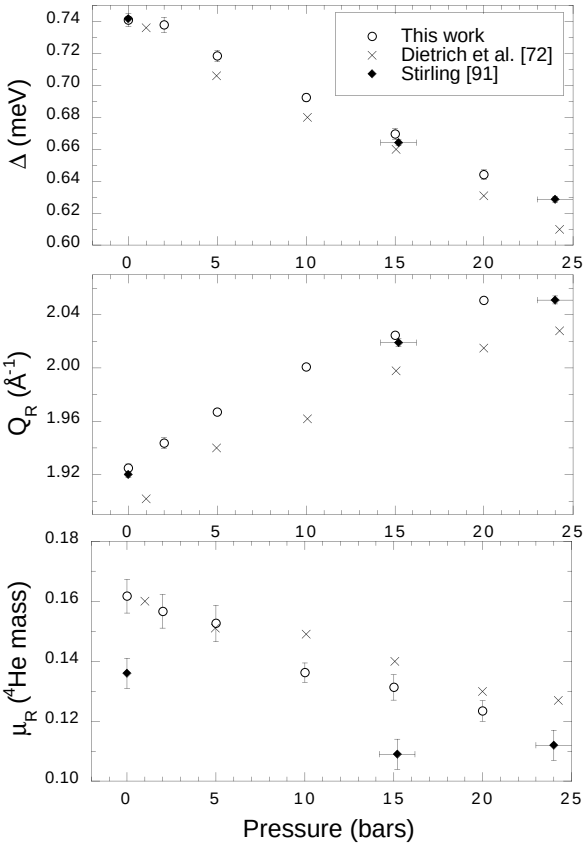

Figure 13. The pressure dependence of the fitted Landau roton parameters Δ, Q_R, and μ_R, at $T = 0.5$ K. Comparison is made with previous studies.

5.3. The pressure dependence of the fitted DHO parameters in the roton region

The lower panel of figure 5 illustrates how the roton excitation energy is dependent on pressure. In agreement with previously observed values [10], the energy decreases with increasing pressure. To obtain more quantitative and useful information about the roton's pressure dependence, the observed excitation energies in this region were fitted to the usual parabolic form first given by Landau [31]:

$$E_Q = \Delta + \frac{\hbar^2(Q - Q_R)^2}{2\mu_R} \tag{3}$$

Table 1. The temperature dependence of the fitted Landau roton parameters Δ, μ_R, and Q_R at pressures up to 20 bar. Excitation energies were extracted using the simple-subtraction method (see the text).

Pressure (bar)	Temperature (K)	Δ (meV)	dΔ (meV)	μ_R (^{4}He mass)	dμ_R (^{4}He mass)	Q_R (Å^{-1})	dQ_R (Å^{-1})
SVP	0.50	0.743	0.002	0.161	0.004	1.929	0.002
SVP [19]	0.05	0.742	0.001	0.136	0.005	1.920	0.002
SVP [19]	0.90	0.742		0.150		1.924	
SVP [19]	0.75	0.743	0.001	0.126	0.03	1.926	0.005
SVP [19]	'Low'	0.742		0.153		1.93	
SVP [AS]	1.24	0.743	0.002	0.142	0.003	1.929	0.003
2	0.50	0.734	0.003	0.160	0.004	1.946	0.002
5	0.50	0.718	0.004	0.153	0.006	1.967	0.003
5	1.40	0.712	0.003	0.154	0.007	1.970	0.003
5	1.60	0.702	0.004	0.153	0.007	1.970	0.003
5	1.80	0.683	0.004	0.150	0.006	1.970	0.003
5	1.95	0.659	0.005	0.146	0.008	1.975	0.003
5	2.00	0.645	0.006	0.142	0.008	1.978	0.004
5	2.05	0.630	0.007	0.142	0.01	1.985	0.004
5	2.10	0.599	0.009	0.137	0.014	1.996	0.007
5	2.15	0.555	0.013	0.135	0.016	2.011	0.011
5	2.20	0.533	0.014	0.132	0.016	2.015	0.016
5	2.50	0.494	0.015	0.125	0.015	2.024	0.013
10	0.50	0.692	0.002	0.130	0.003	2.005	0.001
10	1.40	0.684	0.002	0.136	0.003	2.002	0.002
10	1.60	0.673	0.003	0.137	0.003	2.002	0.002
10	1.80	0.649	0.003	0.135	0.004	2.005	0.002
10	1.95	0.611	0.006	0.126	0.006	2.001	0.003
10	2.00	0.589	0.006	0.120	0.006	2.002	0.003
10	2.05	0.545	0.010	0.109	0.008	2.023	0.005
10	2.10	0.490	0.016	0.102	0.010	2.037	0.007
10	2.15	0.456	0.020	0.099	0.011	2.043	0.009
10	2.50	0.433	0.025	0.094	0.012	2.041	0.008
15	0.50	0.668	0.002	0.123	0.003	2.029	0.002
15.06 [10]	1.28	0.660		0.14		1.998	
15.2 $\pm$ 1 [19]	0.90	0.664	0.002	0.109	0.005	2.019	0.003
20	0.50	0.641	0.002	0.112	0.003	2.055	0.002
20	1.40	0.629	0.003	0.122	0.004	2.054	0.002
20	1.60	0.615	0.003	0.122	0.003	2.053	0.002
20	1.70	0.597	0.003	0.120	0.003	2.056	0.002
20	1.75	0.583	0.004	0.118	0.004	2.059	0.002
20	1.80	0.563	0.004	0.113	0.004	2.063	0.002
20	1.85	0.531	0.005	0.105	0.004	2.070	0.002
20	1.90	0.462	0.007	0.090	0.004	2.080	0.003
20	1.95	0.323	0.023	0.072	0.007	2.094	0.007
20	2.00	0.303	0.035	0.073	0.010	2.096	0.009
20	2.50	0.325	0.043	0.089	0.014	2.100	0.010
24.0 $\pm$ 1 [19]	0.90	0.629	0.002	0.112		2.051	0.003
24.26 [10]	1.25	0.6101		0.127		2.028	

where Δ is the roton energy gap, Q_R is the wavevector of the roton minimum, and μ_R is the effective roton mass. This parabola fits the excitation energies well in the region $Q_R \pm 0.2$ Å^{-1}. Figure 13 shows the pressure dependence of these roton parameters, and they are also listed in table 1. A systematic discrepancy is noted between the roton data presented in this study and the pressure-dependent data of Dietrich *et al* [10]: both Δ and Q_R are consistently higher and μ_R is consistently lower. More recent data presented by Stirling [19] are, however, in closer agreement with the data presented here (except for μ_R). It can be concluded therefore that, although Dietrich *et al* [10] indicated the general trends of the roton's pressure dependence, advances in neutron scattering techniques and analysis since their study have led to a more accurate determination of the Landau roton parameters, shown here and by Stirling [19].

Many theoretical studies using correlated basis-function methods indicate that, contrary to experimental observation, Δ should *increase* with pressure [32]. Recent shadow wavefunction calculations [33, 34], however, show characteristics in agreement with experimental observations of the pressure dependence of Δ. The vast majority of theoretical interpretations have, however, concentrated on the case at SVP [2, 3]. The roton wavevector, Q_R, increases with pressure (figure 13, centre panel). This dependence agrees with the Feynman–Bijl relation $E_Q = \varepsilon_R / S(Q)$ (where ε_R is the free-atom recoil energy), and simple expectations of the density dependence of $S(Q)$. Under pressure, the mean interatomic distance d_0 is expected to decrease. Hence, generally, the dispersion relation E_Q will reach a minimum at the wavevector where $S(Q)$ reaches a maximum.

6. The temperature dependence of the fitted DHO parameters at pressure

The temperature dependences of the single-excitation energies E_Q at 20 bar pressure are shown in figure 14. The temperatures shown are 0.5 K (where the excitation energies are—to within experimental errors—at their $T = 0$ K values), just below T_λ (1.9 K), and above T_λ (2.5 K). The most significant changes to the excitation energies occur in the superfluid phase just below the λ-transition. Above T_λ, the excitations vary little with temperature, and this is true at all pressures. At low temperatures in the superfluid phase, the excitations in the roton region are well defined. On passing through the λ-transition, the roton 'softens' and becomes very broad (see figure 6, lower panel). At 20 bar the excitation energy E_Q at the roton wavevector, obtained using the SS method, is zero in the normal-fluid phase.

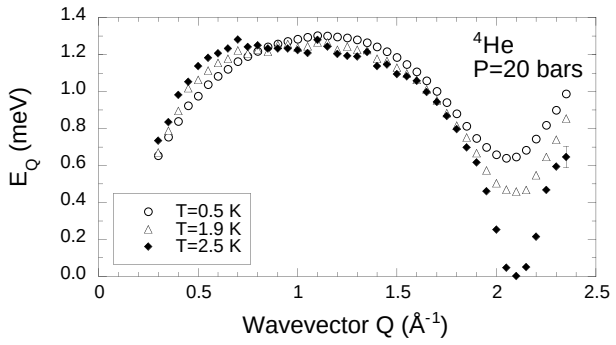

Figure 14. The effect of temperature on the single-excitation energies E_Q at $P = 20$ bar. The energies at low temperature (0.5 K), just below T_λ (1.9 K), and above T_λ (2.5 K) are shown. The data shown at temperatures above 1.9 K, between $0.7 < Q < 1.6$ Å^{-1}, have limited physical meaning as the fitted lineshapes in this region are poor (see section 4.2).

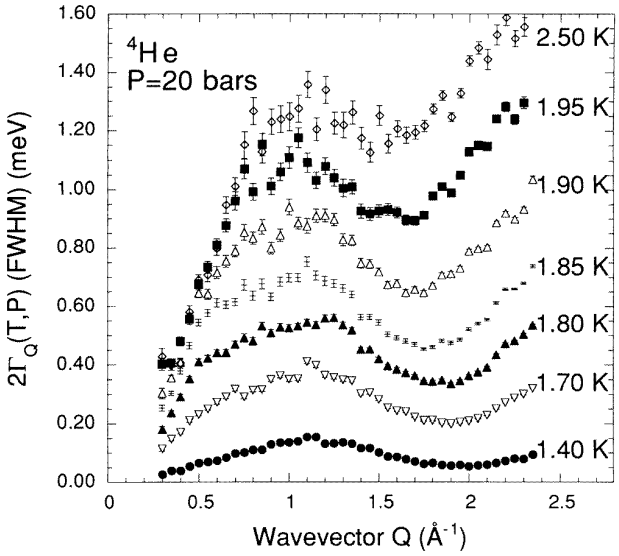

Figure 15. The wavevector dependence of the single-excitation full width at half-maximum (FWHM) linewidths $2\Gamma_Q$ at 20 bar, at various temperatures below and above T_λ. The data shown at temperatures above 1.9 K, between $0.7 < Q < 1.6$ Å^{-1}, have limited physical meaning as the fitted lineshapes in this region are poor (see section 4.2).

The wavevector dependence of the excitation width $2\Gamma_Q$ is shown, at various temperatures, at 20 bar in figure 15. Generally, the excitations broaden more rapidly with temperature at pressure. The general characteristics of the wavevector dependence of $2\Gamma_Q$ do not vary with pressure; the widths remain highly wavevector dependent for $T > 1.5$ K at all pressures. The single-excitation widths at all temperatures (including SVP [AS]) and pressures tend towards zero as $Q \to 0$. This remains true above T_λ. Although very high-resolution measurements have been made of the excitations revealing the excitation widths to a very high degree of accuracy [35, 36], these measurements do not extend to higher pressures. It is hoped that this will be an area of future investigation.

The individual temperature dependencies of the DHO parametrization in the phonon, maxon, and roton regions are discussed below.

6.1. The temperature dependence at pressure of the fitted DHO parameters in the phonon region

The temperature dependence of the phonon data ($Q = 0.4$ Å^{-1}) at 20 bar was shown in the upper panel of figure 6. The fitted DHO parameters of the single excitations (extracted using the simple-subtraction method) are shown in figure 16. The single-phonon parameters have a significant temperature dependence. The temperature dependence of the phonon excitation energy E_Q is shown in the upper panel of figure 16. As the λ-transition is approached, the excitation energy increases. The increase is more pronounced at higher pressure. This shift in energy can also be seen in the raw data (figure 6, upper panel) and is not, therefore, a product of the fitting routine. Above T_λ, the excitation energies are largely independent of temperature at all pressures. When the helium is at SVP, at temperatures higher than 2.5 K the phonon excitation energy decreases [30]; it is expected that the excitation energies at pressure would behave similarly at these temperatures.

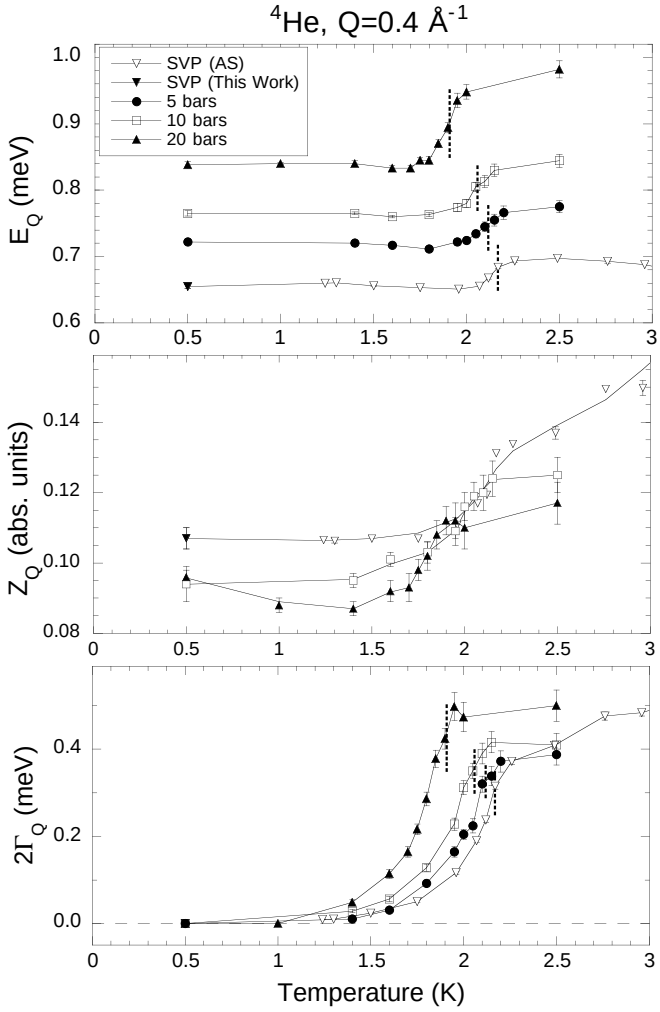

Figure 16. The temperature dependence of the single-excitation energies E_Q (upper panel), weights in $S(Q, E)$, Z_Q (centre panel; for clarity the 5 bar data are not shown), and linewidths $2\Gamma_Q$—full width at half-maximum—(lower panel), in the phonon region ($Q = 0.4$ Å^{-1}) at various pressures. The lambda transition temperature, at each pressure, is indicated by the dotted lines. The solid curves are a guide to the eye.

The substantial change in the phonon energy at the λ-transition, when the helium is at pressure (figure 6, upper panel and figure 16, upper panel), is significant in the context of the Glyde–Griffin model [2, 3, 16, 37]. In the normal-fluid phase, $S(Q, E)$ is dominated by a broad zero-sound peak which is not very temperature dependent. The zero-sound mode is not dependent on a Bose condensate. Below T_λ, in the superfluid phase, $S(Q, E)$ begins to exhibit a new resonance associated with single-particle excitations as a result of a condensate-induced hybridization [2]. The weight of this quasiparticle mode scales with the Bose condensate fraction.

At SVP a much smaller change to the phonon energy is observed at the λ-transition than at pressure. At increased pressure, the more marked changes at T_λ indicate a 'separation'

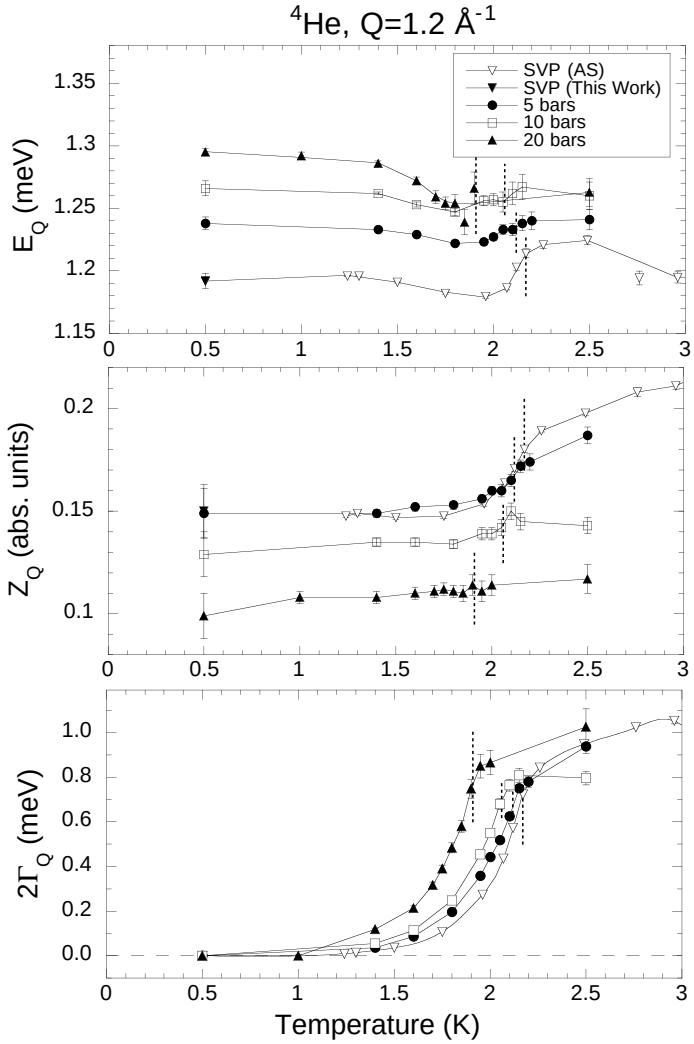

Figure 17. The temperature dependence of the single-excitation energies E_Q (upper panel), weights in $S(Q, E)$, Z_Q (centre panel), and linewidths $2\Gamma_Q$—full width at half-maximum—(lower panel), in the maxon region ($Q = 1.2$ Å^{-1}) at various pressures. The lambda transition temperature, at each pressure, is indicated by the dotted curves. The solid curves are a guide to the eye. The data shown at temperatures above 1.9 K have limited physical meaning as the fitted lineshapes in this region are poor (see section 4.2).

between the single-quasiparticle (condensate-related) mode and the zero-sound (condensate-independent) mode. At these higher pressures, the temperature dependence of the phonon ($Q = 0.4$ Å^{-1}) excitation is more similar to that of excitations at higher (maxon–roton) wavevectors than at SVP.

The effect of pressure on the variation with temperature of the single-excitation weight Z_Q in the phonon region is unremarkable (figure 16, centre panel). Z_Q does not change abruptly at the λ-transition at any pressure. Below 1.5 K the phonon excitation width remains very narrow at all pressures (figure 16, lower panel). Nearer the λ-transition the phonon broadens significantly. The rate of broadening with temperature ($\mathrm{d}\Gamma_Q/\mathrm{d}T$) just below the λ-transition is

greater at higher pressure. Above T_λ, the phonon widths remain almost constant at all pressures. So, as with the phonon energy, the phonon linewidth (lifetime) changes more rapidly close to T_λ.

6.2. The temperature dependence at pressure of the DHO fitted parameters in the maxon region

The temperature dependence at pressure of $S(Q, E)$ in the maxon region ($Q = 1.2$ Å^{-1}) was shown in the centre panel of figure 6; great similarity is seen with the SVP data of AS. The temperature dependence of the excitation energy E_Q is shown in the upper panel of figure 17. The single-excitation energies at SVP, 5 bar, and 10 bar are relatively constant below $T_\lambda - 0.2$ K. Above this temperature the energies increase to reach their respective values at T_λ, where they remain constant in the normal fluid. At 20 bar, however, the energies decrease slightly with temperature with an increased uncertainty in excitation energy near T_λ. This increased uncertainty is believed to be due to the inaccuracy of the SS extraction of the single excitation from $S(Q, E)$; at higher pressures the multiphonon contribution to $S(Q, E)$ is more significant and overlaps considerably with the single excitation in the maxon region. The extracted single-maxon excitation lineshape is, therefore, less well represented by the DHO function at higher temperatures. The single-excitation weight Z_Q at the maxon is shown in the centre panel of figure 17. Z_Q diminishes with increasing pressure at all temperatures, as is consistent with expectations of increasing single-phonon/multiphonon hybridization. Although Z_Q increases slightly with temperature, there are no large changes which can be related to the λ-transition. The temperature variation of the single-excitation widths at the maxon is shown, at several pressures, in the lower panel of figure 17. Although the single-excitation widths $2\Gamma_Q$ in this region are generally broader than those in the phonon region, their qualitative characteristics are similar.

6.3. The temperature dependence of the DHO fitted parameters in the roton region

The lower panel of figure 6 shows the temperature dependence, at 20 bar, of the observed $S(Q, E)$ at the roton wavevector ($Q = 2.0$ Å^{-1}). At pressure, the roton excitation is seen to broaden with increasing temperature below T_λ, at pressure, and at SVP (AS). Above T_λ there is very little change to the excitation. The temperature dependencies of the fitted parameters E_Q, Z_Q, and $2\Gamma_Q$ at the roton wavevector are shown in figure 18; at all temperatures the excitation energy E_Q (upper panel) decreases with increasing pressure. As can be seen, the temperature-dependent characteristics of E_Q are independent of pressure in this region; at low temperatures ($T < T_\lambda - 0.2$ K), E_Q decreases gradually with increasing temperature. As the λ-transition is approached, E_Q diminishes rapidly. Above T_λ, it continues to decrease but does so less rapidly. By contrast, the excitation linewidth $2\Gamma_Q$ increases with pressure at all temperatures. $2\Gamma_Q$ is zero at $T = 0$ K, and increases slowly with temperature below $T_\lambda - 0.2$ K. Above this temperature it increases more rapidly, and above the λ-transition the rate of increase is less. Z_Q is larger at higher pressure and appears to increase rapidly as the temperature approaches the λ-transition. This is believed to be an artefact of the DHO fitting function producing a singularity in Z_Q as $E_Q \to 0$.

The Landau roton parabola (equation (3)) was fitted to the excitation energies at elevated temperature, which gave the temperature dependences of Δ, μ_R, and Q_R at pressure. These values are listed in table 1.

As stated earlier, Δ is smaller at increased pressure. This remains the case at all temperatures. Dietrich *et al* [10] showed that the temperature dependence of Δ follows the

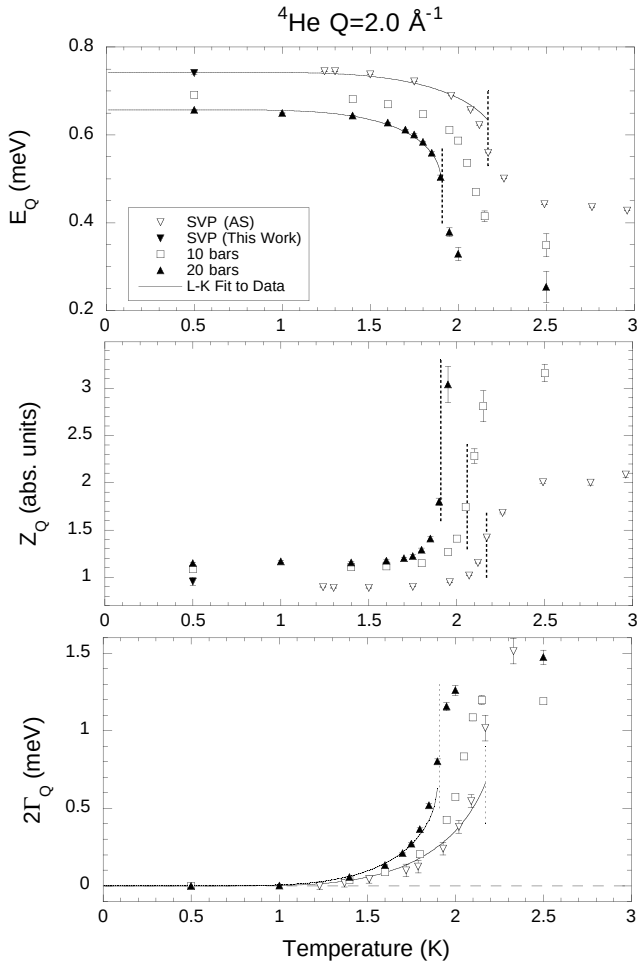

Figure 18. The temperature dependence of the single-excitation energies E_Q (upper panel), weights in $S(Q, E)$, Z_Q (centre panel), and linewidths $2\Gamma_Q$—full width at half-maximum—(lower panel), in the roton region ($Q = 2.0$ Å^{-1}) at various pressures. The solid curves show a least-squares fit of the Landau–Khalatnikov free-excitation-gas model (see the text) to the experimental data. The lambda transition temperature, at each pressure, is indicated by the dotted lines. For clarity, the 5 bar data are not shown.

same universal curve of T_λ–T versus $\Delta(T)$–$\Delta(0)$ at all pressures; this was found to be true for the data in this study. Significant deviations were, however, found from this universal behaviour near the λ-transition, and these may be caused by the difficulty of defining excitation energies near T_λ where the excitations are broad.

At SVP, Q_R is nearly independent of temperature. However, at increased pressure, although Q_R remains constant up to $T_\lambda - 0.2$ K, it increases close to the λ-transition. This increase is attributed to the fact that each measurement was made, with incremental temperature, by keeping the pressure and not the density constant. The density of superfluid ^{4}He increases along an isobar. The roton mass μ_R has a similar temperature dependence at pressure and this may also be attributed to the same effect.

The Landau–Khalatnikov forms of the temperature dependences of the roton linewidth

$2\Gamma_R$ and Δ are shown in equation (4) (least-squares fits of this form to the observed parameters at each pressure are shown in figure 18):

$$\begin{aligned} \Gamma_R &\propto \sqrt{T}\exp(\Delta/k_BT) \\ \Delta(0) - \Delta(T) &\propto \sqrt{T}\exp(\Delta/k_BT). \end{aligned} \tag{4}$$

The Landau–Khalatnikov theory models the temperature dependence of a weakly interacting (Bose) roton gas. At higher densities, interactions between excitations are expected to be stronger, and a roton liquid theory [38] would be more applicable. However, the fitted curves in figure 18 indicate that the Landau–Khalatnikov form describes the data adequately at higher pressure.

The temperature dependence of the roton excitation width $2\Gamma_R$ is shown in the lower panel of figure 18. $2\Gamma_R$ increases with temperature at all pressures in agreement with previous studies [10, 15, 25]. The rate of increase, $\mathrm{d}\Gamma_R/\mathrm{d}T$, increases with pressure corresponding to a decrease in roton lifetime—expected in a more dense fluid. Apparent deviations from Landau–Khalatnikov behaviour of $2\Gamma_R$ at higher temperatures are more likely to reflect the inadequacy of the SS model in extracting single-phonon parameters than any inherent inaccuracy of the Landau–Khalatnikov model.

7. Multiphonon excitations

At energies higher than those of the single-phonon–roton excitations, considerable multiphonon structure is observed in $S(Q, E)$ at low temperatures. This additional structure is caused by the creation of more than one excitation in a single-scattering event. The structure of the multiphonon continuum is related to the two-phonon density of states.

Several studies have been made of the multiphonon scattering. Initial measurements were made by Cowley and Woods [25] and then later studies were made by Svensson and co-workers [13]. The multiphonon excitations of helium at pressure were investigated by Dietrich *et al* [10] and Graf *et al* [12]. In all of these studies the instrumental resolution was inadequate to distinguish separate contributions to the multiphonon structure. More recent measurements at SVP and at pressure by Talbot *et al* [15], Stirling and Glyde [20], Stirling [39], and Crevecoeur *et al* [40] have employed better-resolution conditions and revealed structure to the multiphonon excitations. Although the scattering observed in these studies is broad, clear peaks can be distinguished corresponding to the excitation of two rotons (2R), two maxons (2M), and a maxon and a roton (M + R). These two-particle excitation processes are believed to play a dominant role due to the high density of states at the maxon and the roton.

Theoretical studies of the multiphonon excitations have been made. Götze and Lücke [41] model the excitations within the Mori formalism, and Manousakis and Pandharipande [42] use a correlated basis-function method. Both of these studies show significant multiphonon structure with resonances arising from two rotons ($E_{SVP} \approx 1.5$ meV), two maxons ($E_{SVP} \approx 2.4$ meV), and a maxon plus a roton ($E_{SVP} \approx 1.9$ meV). Manousakis and Pandharipande [42] show that between 0.8 $\text{Å}^{-1}$and 1.9 Å^{-1}, a strong peak is observed at the M + R energy with weaker side peaks associated with 2R and 2M excitations. Stirling [39] showed that this is in broad agreement with the data at SVP. Comparison to the theoretical studies is limited because not only do they not extend to pressure above SVP, but also because the shape of the multiphonon spectrum depends strongly on the number of self-energy terms included in the calculation. In the work of Manousakis and Pandharipande [42] only the first three terms have been included.

The pressure dependences of the multiphonon excitations at 0.5 K, at 20 bar, at the phonon, maxon, and roton are shown in figure 19. The multiphonon contribution in the phonon region ($Q = 0.4$ Å^{-1}) is relatively small (<5% of the single-excitation peak strength). Although

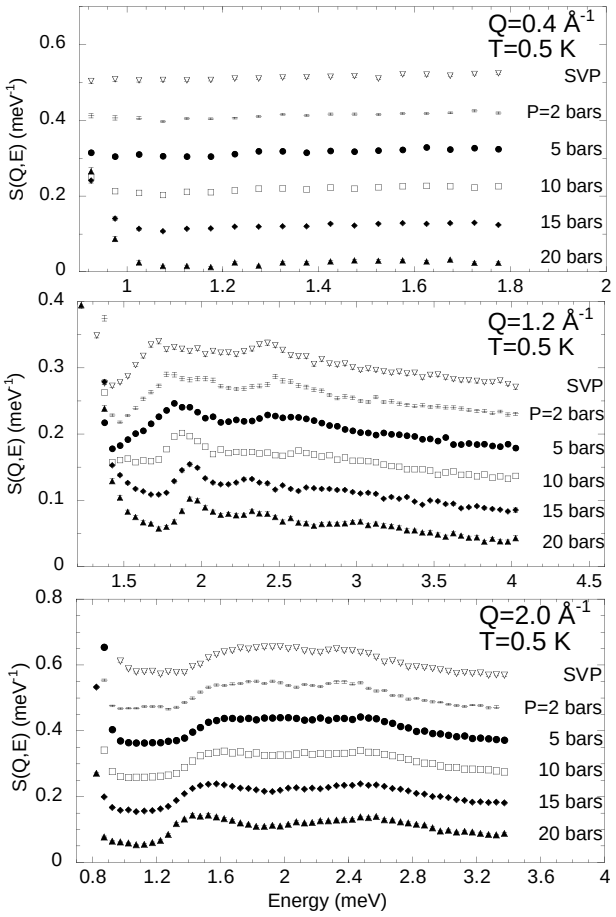

Figure 19. Low-temperature (0.5 K) constant-Q scans of $S(Q, E)$ of ^{4}He at the phonon ($Q = 0.4$ Å^{-1}), maxon ($Q = 1.2$ Å^{-1}), and roton ($Q = 2.0$ Å^{-1}) at various pressures, emphasizing the multiphonon excitations. For clarity, the data at each pressure have been shifted by 0.02 meV^{-1} in the upper panel, 0.05 meV^{-1} in the centre panel, and 0.1 meV^{-1} in the lower panel. The 20 bar data in each case are not shifted.

little structure is observed, it can be seen that the multiphonon contribution at higher pressure is centred at $E \approx 1.55$ meV in a broad single peak. This peak is not so clearly observed at SVP [4, 5].

In the maxon region ($Q = 1.2$ Å^{-1}), the changes with pressure in the multiphonon region are more apparent. The first peak of the multiphonon structure at this wavevector is centred at $E \approx 1.7$ meV at SVP and increases to 1.9 meV at 20 bar; this arises principally from a maxon + roton (M + R) feature. The strength of the multiphonon excitations in the maxon region is approximately independent of pressure.

At the roton wavevector ($Q = 2.0$ Å^{-1}) the magnitude of the multiphonon component is roughly twice that observed in the maxon region. More detailed structure is seen at higher pressure. The broad single peak observed at SVP (centred at $E \approx 2$ meV) bifurcates with pressure and, at 20 bar, two distinct peaks can be resolved in the multiphonon; the first at twice the roton energy (2R), the second at twice the maxon energy (2M). At SVP the 2R

and 2M energies are closer together and the separate peaks cannot be resolved. Although individual 'peak positions' may be resolved in the multiphonon component at higher pressure, it is misleading to view these as two separate and distinct components. The phonon–maxon–roton dispersion relation is continuous, and the multiphonon 'continuum' is made up of the sum of an infinite variety of possible combinations of single excitations. In the 20 bar data we observe a single-multiphonon continuum with two maxima in intensity. A broad continuum of scattering is seen in the multiphonon at all wavevectors at higher energies. Although $S(Q, E)$ is predicted to decrease in intensity at high energies with a $E^{-7/2}$-dependence [43], the energy range studied was not large enough to confirm this.

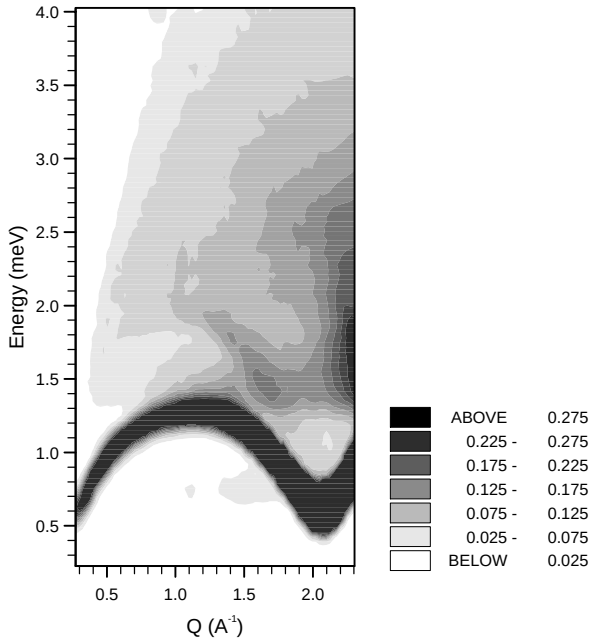

Figure 20. A contour plot showing the multiphonon excitations in ^{4}He at $T = 0.5$ K, $P = 20$ bar. The single-phonon–roton excitations have been removed to reveal the multiphonon structure. The feature below the single excitations at $Q \approx 1.5$ Å^{-1}, $E = 0.75$ meV is due to multiple scattering of single rotons and Bragg scattering from the aluminium sample cell.

Figure 20 shows a contour map of the multiphonon excitations at $T = 0.5$ K, $P = 20$ bar. The full height of the single, sharp excitations has been 'chopped off', revealing the dependence of Q and E of the (considerable) multiphonon structure. In the maxon region, a strong M + R feature is observed. This feature is also observed at SVP [39], and is also predicted in theory [42].

At roton wavevectors a 'ridge' of scattering is seen in the roton region when $E = 2$R. This two-roton ridge coincides with the single-excitation peak at $Q \approx 1.5$ Å^{-1}, and this merging may result in strong anharmonic crossover effects between the single-phonon and multiphonon excitations. This two-roton ridge also coincides with the single excitations at wavevectors higher than that of the roton. This may lead to the observed 'bending over' of the excitations to approximately 2Δ at wavevectors beyond that of the roton [44, 45].

8. Conclusions

The collective excitations in normal and superfluid ^{4}He have been investigated as functions of both pressure and temperature. A number of interesting results have arisen from this study, for example the increased change of the phonon energy—at pressure—upon passing thorough the λ-transition. This quantitative result indicates that the phonon excitation changes more on passing from the normal to the superfluid phases than had been previously thought on the evidence of SVP data alone [20]. In addition to the change in the phonon energy, this work has confirmed the importance of multiphonon excitations in the dynamics of liquid helium.

It is hoped that these results will provide a stimulus to the ongoing debate on the origin of the excitations and their relation to the Bose–Einstein condensate. Indeed, a comparison between the data presented here and the Glyde–Griffin density–quasiparticle model [16] is in preparation. The density–quasiparticle model links the collective excitations to the Bose condensate.

Taken with the study of AS, precision measurements have now covered much of the liquid phase diagram. While compilations are available of the many previous neutron scattering studies to date (see for example Donnelly *et al* [46]), the results presented in this study—combined with those of AS—are self-consistent and were taken under very similar experimental conditions.

Acknowledgments

This work was supported by the Engineering and Physical Sciences Research Council. We acknowledge the technical assistance of staff at the ILL.

References

[1] Landau L D 1941 *Phys. Rev.* **60** 356
[2] Griffin A 1993 *Excitations in a Bose Condensed Fluid (Cambridge Studies in Low Temperature Physics vol 4)* ed A M Goldman, P V E McClintock and M Springford (Cambridge: Cambridge University Press)
[3] Glyde H R 1995 *Excitations in Liquid and Solid Helium (Oxford Series on Neutron Scattering in Condensed Matter vol 9)* ed S W Lovesey and E W J Mitchell (Oxford: Oxford University Press)
[4] Andersen K H, Stirling W G, Scherm R, Stunault A, Fåk B, Godfrin H and Dianoux A J 1994 *J. Phys. C: Solid State Phys.* **6** 821
[5] Andersen K H and Stirling W G 1994 *J. Phys. C: Solid State Phys.* **6** 5805
[6] Svensson E C, Montfrooij W and de Schepper I M 1996 *Phys. Rev. Lett.* **77** 4398
[7] Crevecoeur R M 1996 *PhD Thesis* Delft University of Technology
[8] Miller A, Pines D and Nozières P 1962 *Phys. Rev.* **127** 1452
[9] Woods A D B and Svensson E C 1978 *Phys. Rev. Lett.* **41** 974
[10] Dietrich O W, Graf E H, Huang C H and Passell L 1972 *Phys. Rev.* A **5** 1377
[11] Woods A D B and Cowley R A 1973 *Rep. Prog. Phys.* **36** 1135
[12] Graf E H, Minkiewicz V J, Bjerrum Møller H and Passell L 1974 *Phys. Rev.* A **10** 1748
[13] Svensson E C, Martel P, Sears V F and Woods A D B 1976 *Can. J. Phys.* **54** 2178
[14] Svensson E C, Woods A D B and Martel P 1972 *Phys. Rev. Lett.* **29** 1148
[15] Talbot E F, Glyde H R, Stirling W G and Svensson E C 1988 *Phys. Rev.* B **38** 11 229
[16] Glyde H R and Griffin A 1990 *Phys. Rev. Lett.* **65** 1454
[17] Gibbs M R 1996 *PhD Thesis* Keele University
[18] Buyers W J L, Sears V F, Lonngi P A and Lonngi D A 1975 *Phys. Rev.* A **11** 697
[19] Stirling W G 1991 *Excitations in Two-Dimensional and Three-Dimensional Quantum Fluids* ed A F G Wyatt and H J Lauter (New York: Plenum) p 25
[20] Stirling W G and Glyde H R 1990 *Phys. Rev.* B **38** 11 229
[21] Cowley R A 1968 *Rep. Prog. Phys.* **31** 123

[22] Fåk B and Dorner B 1992 On the interpretation of phonon line shapes and excitation energies in neutron scattering experiments *Institut Laue–Langevin Internal Report*
[23] Tarvin J A and Passell L 1979 *Phys. Rev.* B **36** 1458
[24] Andersen K H 1991 *PhD Thesis* Keele University
[25] Cowley R A and Woods A D B 1971 *Can. J. Phys.* **49** 177
[26] Griffin A and Svensson E C 1990 *Physica* B **165+166** 487
[27] Maynard J 1976 *Phys. Rev.* B **14** 3868
[28] Aldrich C H III, Pethick C J and Pines D 1976 *Phys. Rev. Lett.* **37** 845
[29] Glyde H R and Svensson E C 1987 *Methods of Experimental Physics* vol 23, ed D L Price and K Sköld (New York: Academic) ch 13
[30] Svensson E C, Martel P and Woods A D B 1975 *Phys. Lett.* A **25** 151
[31] Landau L D 1947 *J. Phys. USSR* **11** 91
[32] Padmore T C and Chester G V 1974 *Phys. Rev.* A **9** 1725
[33] Wu W, Vitiello S A, Reatto L and Kalos M H 1991 *Phys. Rev. Lett.* **67** 1446
[34] Reatto L, Vitiello S A and Masserini G L 1993 *J. Low Temp. Phys.* **93** 879
[35] Mezei F and Stirling W G 1983 *75th Jubilee Conf. on Helium-4* ed J G M Armitage (Singapore: World Scientific) p 111
[36] Andersen K H, Bossy J, Cook J C, Randl O G and Ragazzoni J L 1996 *Phys. Rev. Lett.* **77** 4043
[37] Glyde H R 1992 *Phys. Rev.* B **45** 7321
[38] Bedell K, Pines D and Zawadowski A 1984 *Phys. Rev.* B **29** 102
[39] Stirling W G 1990 *Physica* B **165+166** 501
[40] Crevecoeur R M, Smorenburg H E, de Schepper I M, Montfrooij W and Svensson E C 1996 *Czech. J. Phys.* **46** 257
[41] Götze W and Lücke M 1976 *Phys. Rev.* B **13** 3825
[42] Manousakis E and Pandharipande V R. 1986 *Phys. Rev.* B **33** 150
[43] Family F 1975 *Phys. Rev. Lett.* **34** 1374
[44] Pitaevskii L P 1959 *Sov. Phys.–JETP* **9** 830
[45] Glyde H R, Gibbs M R, Stirling W G and Adams M A 1998 *Europhys Lett.* **43** 422
[46] Donnelly R J, Donnelly J A and Hills R N 1981 *J. Low Temp. Phys.* **44** 471